ResearchGate

See discussions, stats, and author profiles for this publication at: https://www.researchgate.net/publication/231643356

Molecular Dynamics Study on Diameter Effect in Structure of Ethanol Molecules Confined in Single-Walled Carbon Nanotubes

ARTICLE *in* THE JOURNAL OF PHYSICAL CHEMISTRY C · NOVEMBER 2007

Impact Factor: 4.77 · DOI: 10.1021/jp0736140

CITATIONS
30

READS
52

10 AUTHORS, INCLUDING:

Qing Shao
University of Washington Seattle
31 PUBLICATIONS **499** CITATIONS
SEE PROFILE

Liangliang Huang
University of Oklahoma
26 PUBLICATIONS **346** CITATIONS
SEE PROFILE

Linghong Lu
Nanjing University of Technology
46 PUBLICATIONS **615** CITATIONS
SEE PROFILE

Keith E Gubbins
North Carolina State University
200 PUBLICATIONS **7,329** CITATIONS
SEE PROFILE

Available from: Jian Zhou
Retrieved on: 26 January 2016

Molecular Dynamics Study on Diameter Effect in Structure of Ethanol Molecules Confined in Single-Walled Carbon Nanotubes†

Qing Shao,‡ Liangliang Huang,‡ Jian Zhou,§ Linghong Lu,‡ Luzheng Zhang,|| Xiaohua Lu,*,‡ Shaoyi Jiang,⊥ Keith E. Gubbins,# Yudan Zhu,‡ and Wenfeng Shen‡

State Key Laboratory of Materials-oriented Chemical Engineering, Nanjing University of Technology, Nanjing 210009, P. R. China, School of Chemical and Energy Engineering, South China University of Technology, Guangzhou 510640, P. R. China, Petroleum Research Recovery Center, New Mexico Institute of Mining and Technology, Socorro, New Mexico 87801, Department of Chemical Engineering, University of Washington, Seattle, Washington 98195, and Department of Chemical and Biomolecular Engineering, North Carolina State University, Raleigh, North Carolina 27695-7905

Received: May 11, 2007; In Final Form: July 9, 2007

Equilibrium molecular dynamics simulations have been performed to investigate the structural characteristics of ethanol molecules confined in single-walled, pristine armchair carbon nanotubes with a length of 2.5 nm and diameters ranging from 0.68 to 1.35 nm in an open ethanol reservoir at 298.0 K and 100.0 kPa by all-atom and united-atom models. Both models present similar results. Structural properties of confined ethanol molecules are analyzed in terms of the average number of hydrogen bonds, radial density distributions of methyl and hydroxyl groups, orientation distributions of the methyl−methylene bond, oxygen−hydrogen bond and dipole moment, and molecular conformations as a function of the diameter of carbon nanotubes. The results indicate that the behavior of the nonpolar part of confined ethanol molecules changes monotonically with the diameter, whereas that of the polar part changes non-monotonically. The different dependence on diameter indicates that the wall−fluid interactions determine the behavior of nonpolar groups, whereas that of polar groups is determined by the fluid−fluid interactions. Only in the nanotube with a diameter of 1.081 nm did the confined ethanol molecules have a highly preferred dipole orientation. The conformational equilibrium also varies considerably with the diameter non-monotonically. The largest proportion of gauche ethanol corresponds to the most preferred dipole orientation.

I. Introduction

The behavior of molecules confined in the nanopore is currently a subject of great interest because it plays an important role in many applications such as molecular detection,[1] gas storage,[2] and membrane separation.[3,4] As an important fluid in both chemical and biological fields, the behavior of ethanol molecules in nanopores has significant impacts on many biological and chemical processes. Ethanol can modulate the function of the nicotinic receptor. Ethanol molecules are found to place themselves near the hydrophobic domain of the pore[5] and block the ion flux within the channel, causing many of the well-known effects of alcohol in humans, such as behavior disorder or anesthesia. The modulation function of alcohol on many other ion-channels is also suggested to be related with the behavior of ethanol molecules inside the channel pore.[6−8] In addition, the behavior of ethanol within the nanopore is important for the production of fuel-grade ethanol,[9] where the nanoporous material is applied broadly. However, little is known about the molecular-scale behavior of ethanol within the nanopore, experimentally.

Nevertheless, molecular simulation offers an alternative approach to this field. Using molecular simulation, Gubbins and his co-workers studied the adsorption and phase equilibrium of simple gas,[10,11] water,[12−14] and mixtures[15,16] within various nanopores. Their studies indicated that the behavior of confined fluids is mainly determined by the anisotropic wall−fluid and fluid−fluid interactions.[17] The change of interactions could result in considerable changes in behavior of the confined fluids. For instance, Hummer et al.[18] found in a molecular dynamics (MD) simulation that a slight reduction in the attraction between the wall and water can lead to sharp, two-state transitions between empty and filled states in a (6, 6) carbon nanotube (CNT). Furthermore, the synergistic effect of the two interactions could induce anomalous behavior of confined fluids. For example, MD simulations have revealed that water molecules confined in CNTs could have characteristic structures. Koga et al.[19] reported MD simulations where water molecules encapsulated in CNTs with diameters ranging from 1.1 to 1.4 nm had new ice phases not seen in bulk ice under pressures of 0.2−0.5 GPa and temperatures of 230−300 K. Recently, Bai et al.[20] found in MD simulations that water molecules inside a (17, 0) CNT would consist of double helixs, which resemble the double helixs of DNA under 250 K and 4 GPa. The MD simulations of Noon et al.[21] and Mashl et al.[22] found that water molecules could also form ice-like structures inside CNTs with proper diameters under the ambient condition. De Souza et al.[23] investigated the structure of water molecules confined in CNTs with neutron-scattering and MD simulations. They found that water molecules

† Part of the "Keith E. Gubbins Festschrift".

* To whom correspondence should be addressed. E-mail: xhlu@njut.edu.cn, phone: +86-25-83588063, fax: +86-25-83588063.
‡ Nanjing University of Technology.
§ South China University of Technology.
|| New Mexico Institute of Mining and Technology.
⊥ University of Washington.
North Carolina State University.

10.1021/jp0736140 CCC: $37.00 © 2007 American Chemical Society
Published on Web 08/24/2007

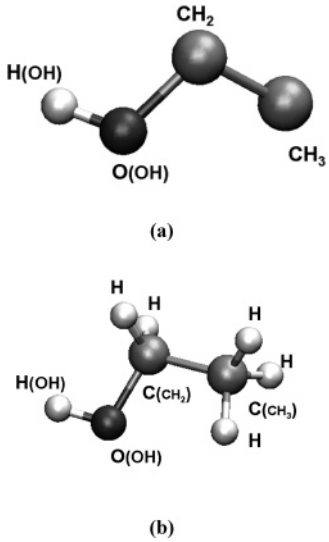

Figure 1. Schematic configurations of (a) the united-atom model and (b) the all-atom model of an ethanol molecule.

formed a square-ice sheet in the CNTs at low temperatures. Huang et al.[24,25] showed in MD simulations that the anchor of carboxyl groups on the mouth of (10, 0) CNT could forbid the entry of water from this end. However, the anchor of carboxyl groups on the mouth of (6, 6) CNT, whose diameter is similar to that of (10, 10) CNT, could not block the entry of water. The enhanced anisotropic interactions induced by the carboxyl groups are suggested to play an important role. Zhou and his co-workers[26] studied the effect of external charge to the water permeation across a carbon nanotube with MD simulations. Their results also indicated that the anisotropic interactions are important for behaviors of confined fluids.

In the case of alcohol molecules, they could form hydrogen bonds as water molecules. Moreover, the coexistence of nonpolar and polar groups makes the interactions of wall−fluid and fluid−fluid more anisotropic. Jiang and his co-workers[27] studied the flow of methanol molecules inside the hydrophobic and hydrophilic pores with nonequilibrium MD simulations. They found that the hydrophilic surface would inevitably change to a "hydrophobic" surface due to the wetting of methanol, which has both hydrophobic methyl and hydrophilic hydroxyl groups. Morineau and his coworkers studied the methanol molecules confined in silica nanopores with neutron scattering analysis[28] and MD simulations.[29] Their results indicated that the hydrogen-bonding interactions of methanol with the surface would have significant influences on the local structure of methanol molecules because there is a nonpolar group on the other side of a methanol molecule. The melting and freezing behaviors of methanol inside a carbon nanopore were also studied.[30] It is found that its melting point is very sensitive to the wall−fluid interaction. As for ethanol, its steric structure is more complex than that of methanol because one ethanol molecule is made up of methyl, methylene, and hydroxyl groups, whereas one methanol molecule has only methyl and hydroxyl groups. Kaneko and his co-workers[31−34] studied the structure of methanol and ethanol confined in carbon nanopores with in situ X-ray diffraction. They found that, although both molecules could form ordered structures within the nanopore, only ethanol had a remarkable preferred orientation. Several molecular simulation studies have been carried out with confined ethanol molecules, including the ethanol within lipid bilayers[35,36] and the ethanol/water mixture in polymeric membranes[37] and zeolites,[38,39] which help gain insight into the performance of ethanol in the nanoporous materials.

TABLE 1: The Lennard−Jones Parameters and Partial Charges for Ethanol Molecule and Carbon Atom of CNT[43,44]

site	σ/nm	ϵ/kJ mol^{-1}	q/e
Ethanol, OPLS united-atom model			
CH_3	0.3775	0.866	0.000
CH_2	0.3905	0.494	0.265
O	0.3070	0.711	−0.700
H	0.0000	0.000	0.435
Ethanol, OPLS all-atom model			
$C(CH_3)$	0.3500	0.276	−0.180
$C(CH_2)$	0.3500	0.276	0.145
$H(CH_3,CH_2)$	0.2500	0.126	0.060
O(OH)	0.3120	0.711	−0.683
H(OH)	0.0000	0.000	0.418
CNT			
C	0.355	0.293	0.000

However, a few critical issues about confined ethanol molecules are not well understood yet. One critical issue is the pore diameter dependence of structural properties of confined ethanol. Theoretical studies have found that structural properties of confined molecules vary considerably with pore diameter, which in turn have significant impacts on their transport[22,40] and phase transition.[19,21] As an anisotropic molecule, the hydrophobic part and the hydrophilic part of ethanol molecules may behave differently in the confinement or alter their behavior differently with the variation of confinement, which would induce some characteristic structure of confined ethanol molecules.

Therefore, we performed MD simulations to investigate the pore diameter effect on structural properties of confined ethanol molecules. The real pores, such as those of biological channels or polymeric membranes, are complicated with irregular surface and highly inhomogeneous charge distributions, making it difficult to investigate the individual effect of pore size. Therefore, we pursue a different strategy to avoid the complexity of biological and industrial systems. We employ the single-walled armchair CNT as the model because recent theoretical studies[18,41] suggested it as a prototype for the complicated 1-dimensional (1D) nanopores. The diameters of CNTs in this study range from 0.68 to 1.35 nm, similar to the size scale of ion-channels. The paper is organized as follows: Section II describes the details of the simulation, and Section III is the discussions of results. On the basis of the discussions in Section III, the main conclusions are in Section IV.

II. Simulation Details

II.A. Molecular Modeling. *Ethanol molecule.* Several models have been developed for ethanol.[42−45] These models could be divided into two categories: the united-atom model, which takes certain group of ethanol as a single interaction site; and the all-atom model that considers each atom as an interaction site. With the proper parameters, the united-atom model could reproduce the bulk properties of ethanol as well as the all-atom model. However, they might produce different results for confined ethanol. To evaluate the sensitivity of the simulation results to the selection of models, we employ both untied-atom and all-atom models in this study. For the united-atom model, OPLS model developed by Jorgensen group[43] is used because the recent theoretical studies[46,47] showed that it can well reproduce the properties of ethanol. The optimized potential for liquid simulations (OPLS) all-atom model,[44] also developed by the Jorgensen group, is employed as the representation of all-

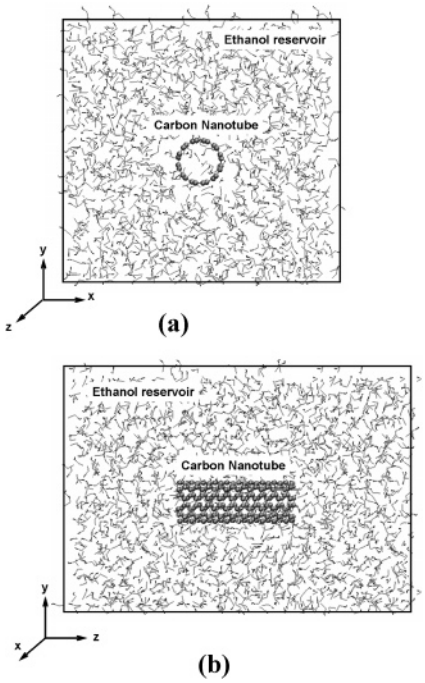

Figure 2. Graphical representation of the simulation cell for the (6, 6) CNT−ethanol, (a) top view and (b) side view.

atom models because of its excellent agreement with experimental results and with the properties of the liquid/vapor interface of ethanol.[48] The OPLS united-atom model places four interaction sites, on the oxygen (O) nuclei, the hydroxyl proton (H) of the hydroxyl group, the united methylene (CH_2) group, and the united methyl (CH_3) group centered on the carbon (C), respectively, whereas the OPLS all-atom model takes every atom of ethanol molecule as an individual interaction site. Figure 1 shows schematic images of these two models.

Carbon nanotube. The single-walled CNT is formed by folding a graphite sheet to a cylinder. Similar to the study of Hummer et al.,[18] each carbon atom of the nanotube is treated as a neutral Lennard−Jones (L−J) interaction site.

The potential energy of intermolecular interactions is described as a combination of a L−J 12−6 potential and a Columbic potential (eq 1),

$$U(r_{ij}) = 4\epsilon_{ij}\left[\left(\frac{\sigma_{ij}}{r_{ij}}\right)^{12} - \left(\frac{\sigma_{ij}}{r_{ij}}\right)^{6}\right] + \frac{q_i q_j}{r_{ij}} \qquad (1)$$

where r_{ij} is the distance between atoms i and j, q_i is the partial charge assigned to atom i, and ϵ_{ij} and σ_{ij} are energy and size parameters obtained by Lorentz−Berthelot combining rules, where $\sigma_{ij} = (\sigma_i + \sigma_j)/2$ and $\epsilon_{ij} = \sqrt{\epsilon_i \epsilon_j}$. Table 1 lists L−J parameters and partial charges used in this study.

II.B. Simulation Method. The ethanol-CNT system was made up of a periodic ethanol box (initial size: 5.0 × 5.0 × 7.0 nm) and a single-walled CNT (2.5 nm in length). The CNT was solvated in a bulk ethanol reservoir and was placed along the *z*-axis in the middle of the box, as illustrated in Figure 2, which were produced with the Visual Molecular Dynamics program (VMD).[49] Initially, ethanol molecules were not placed inside the CNT to make sure that every ethanol molecule enters the pore spontaneously. Table 2 lists the details of 12 simulated systems. The space occupied by CNT is less than 3% of the total volume of the simulation cell, and the ethanol reservoir is proper for the description of the bulk ethanol.

Molecular dynamics simulations were performed in an isobaric−isothermal ensemble (NPT) with a modification of the Groningen machine for chemical simulations (GROMACS, version 3.3.1).[50] For all 12 simulated systems, after the energy minimization and a 1.0 ns MD run with integral steps of 1.0 fs for equilibrium, another 1.0 ns run was carried out with integral step of 2.0 fs, and coordinates were saved every 0.1 ps for analysis. With periodic boundary conditions in all three dimensions, long-range electrostatic interactions were computed with the particle mesh Ewald method,[51] whereas the short-range van der Waals forces were calculated within a cutoff distance of 1.1 nm. The overall system was maintained at 298 K (0.1 ps time constant) and 100.0 KPa with the Berendsen algorithm (with a compressibility of 4.5×10^{-5} bar^{-1} and a 1 ps time constant).[52] Intramolecular bonds of ethanol molecules were kept rigid with the SHAKE algorithm.[53] The bond bending potential is treated harmonically, and the torsional interactions are treated as Fourier series, as described in refs 43 and 44. To keep the diameter of the nanotube steady, carbon atoms of CNT were kept at their initial positions during the MD run. During the production stage, the fluctuation of the potential energy of the ensemble is around 0.5%.

TABLE 2: Simulated Cases for Ethanol−CNT Systems[a]

					N_{in}		Ratio	
(*n*,*n*)	*D*/nm	*N*-UA	*N*-AA	N_C	UA	AA	water (0.28 nm)	ethanol (0.45 nm)
(5, 5)	0.676	1628	1652	200	0.0	0.0	2.46	1.50
(6, 6)	0.811	1617	1649	240	4.0	4.0	2.95	1.80
(7, 7)	0.946	1605	1631	280	5.4	5.4	3.44	2.10
(8, 8)	1.081	1594	1621	320	9.0	8.5	3.93	2.40
(9, 9)	1.216	1587	1612	360	12.6	12.4	4.42	2.70
(10, 10)	1.351	1576	1595	400	16.6	16.7	4.9	3.00

[a] The (*n*, *n*) entries are the CNT's indices; *D* is the CNT's diameter, which is taken from ref 54; *N*-UA and *N*-AA are the numbers of ethanol molecules of the united-atom model and the all-atom model, respectively; *N*c is the number of carbon atom of CNTs; N_{in} is the average occupation number of ethanol in CNTs, for which UA is that for the united-atom model and AA is that for the all-atom model; and the ratio is that between the CNT diameter and the molecular diameter. Properties of bulk ethanol were gained from 500 ps MD run (256 ethanol molecules, 298 *K* at a density of 784 kg m^{-3})

III. Results and Discussions

We found that ethanol molecules could not spontaneously enter the (5, 5) CNT during the MD run. Therefore, results for CNTs with larger diameter are discussed as follows.

III.A. Number of Hydrogen Bonds of Ethanol Molecules in CNTs. The hydrogen-bonding interaction plays a critical role in the behavior of ethanol, similar to that of water. The effect of confinement on the hydrogen-bonding behavior of ethanol molecules is investigated in the term of the average number of hydrogen bonds $<n_{HB}>$. A hydrogen bond is determined by a geometric criterion proposed by Luzar et al.[54] That is to say, two ethanol molecules are considered hydrogen-bonded if the two conditions are fulfilled: (a) the distance between the oxygen (O) sites of two ethanol molecules is shorter than a threshold distance (0.35 nm); and (b) the bond angle between the O−O direction and the molecular O−H (hydroxyl) direction of the donor, where H (hydroxyl) is the hydrogen site that forms the bond, is smaller than a threshold angle (30°). Using this criterion, the $<n_{HB}>$ value of the bulk ethanol is 1.9 according to the united-atom model and 1.87 according to the all-atom model, which are a little larger than the simulation result (1.8) of Jorgensen et al.,[43] who used both energy and geometric criteria. However, it should not affect the variation of $<n_{HB}>$ with the diameter *D*, which is concerned here.

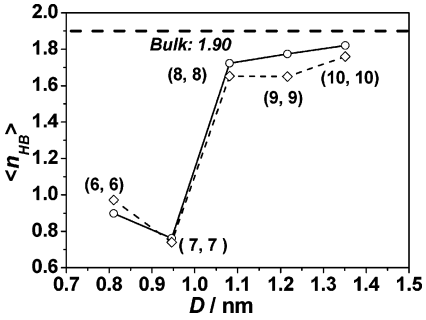

Figure 3. The $<n_{HB}>$ of confined ethanol molecules as a function of tube diameter *D*. (○ : united-atom model; ◇: all-atom model).

Figure 3 shows $<n_{HB}>$ of ethanol molecules within various CNTs. We observe that corresponding results obtained from simulations with united-atom and all-atom models are quantitatively consistent. It is found that $<n_{HB}>$ of ethanol molecules within (8, 8), (9, 9), and (10, 10) CNTs are quite similar, in spite of the increase of diameter. In their MD simulations, Gordillo et al.[55] and Wang et al.[56] found that water molecules confined in CNTs with diameters ranging from 1.0 to 1.5 nm would also have their $<n_{HB}>$ values around 2.4∼2.6, nearly 1.0 less than the bulk counterpart. However, the $<n_{HB}>$ values of confined ethanol molecules within these CNTs is found to be bulk-like. The confinement effect of CNTs with diameters larger than 1.0 nm is little as compared to the $<n_{HB}>$ of ethanol. This might be because of the different spatial requirement of hydrogen bond formation of the water and ethanol molecules. The hydrogen bonds of ethanol molecules do not have the complex tetrahedron structure that water molecules have. Consequently, the spatial requirement to form bulk-like hydrogen bonds is less than that of water molecules, which in turn makes the confinement effect of CNTs with diameters larger than 1.0 nm slight. However, the confinement of CNTs with diameters less than 1.0 nm has obvious effect on $<n_{HB}>$ values of ethanol, similar to that of water molecules.[55,56] From Figure 3, we find that the $<n_{HB}>$ values of ethanol molecules within the (6, 6) and (7, 7) CNTs are around 1.0, indicating that only 50% of the hydrogen bonds of ethanol molecules could be maintained within these two extremely narrow tubes.

III.B. Radial Density Distributions of Methyl and Hydroxyl Groups of Ethanol Molecules within CNTs. The particles have heterogeneous density distribution in the CNT, mainly in the radial direction. As for the ethanol molecule, its polar and nonpolar groups may have different distributions within hydrophobic pores of CNTs. Moreover, their distributions may change differently with diameter. To investigate radial density distributions of nonpolar and polar parts of ethanol molecules within CNTs, radial density profiles (RDPs) of methyl (CH_3) and hydroxyl (OH) groups, in units of the bulk ethanol density ρ_0, were averaged over cylindrical shells centered at the axis of the CNT and were plotted against the cylindrical radius (r).

Figure 4 shows the RDP of CH_3 (RDP-CH_3) and OH (RDP-OH) groups within various CNTs, with results gained from both all-atom and united-atom models. We observed that the RDPs of the united-atom model quantitatively agree with those of the all-atom model, except the RDP-CH_3 in the (6, 6) CNT. The peak height of RDP-CH_3 from the all-atom model (see Figure 4a) is nearly twice that of the united-atom model (see Figure 4b), implying that the effect of model resolution may become significant only within extremely narrow tubes. Nevertheless, both models produce the same peak position for the RDP-CH_3 in (6, 6) CNT. In addition, the peak for the RDP-CH_3 within

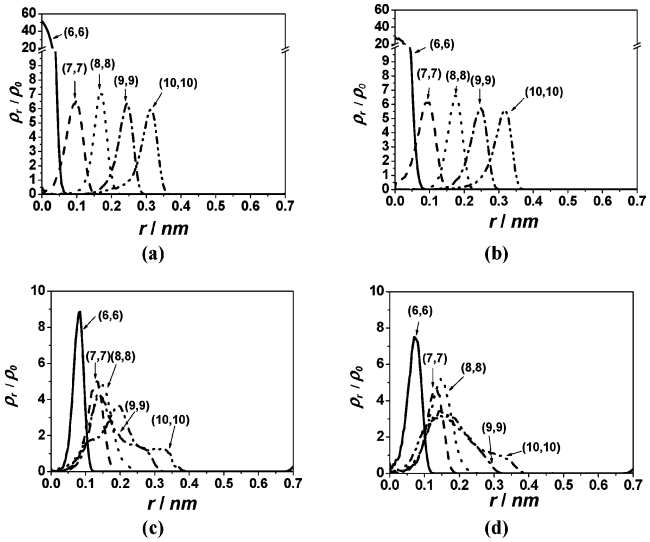

Figure 4. Radial density profiles of methyl and hydroxyl groups of ethanol molecules within various CNTs. (a) Methyl groups (all-atom model); (b) methyl groups (united-atom model); (c) hydroxyl groups (all-atom model); and (d) hydroxyl groups (united-atom model).

the (6, 6) CNT is several orders higher than that within other wider tubes. This indicates the extremely narrow distribution of methyl groups at the axial center of the (6, 6) CNT, which Wang et al.[56] have observed for oxygen RDP of water molecules in the (5, 5) nanotube.

From Figure 4, we also see that shapes of RDP-CH_3 within (7, 7), (8, 8), (9, 9) and (10, 10) CNTs change little with the variation of diameter, whereas those of RDP-OH vary significantly. We investigate variations of RDP-CH_3 and RDP-OH as a function of diameter with two parameters: (a) the peak height h, which characterizes the order of sites within the nanotube; and (b) the peak position d, which is defined as the distance between the CNT wall and peak characterizing the interactions of sites within the nanotube. The smaller d value indicates that the peak is closer to the CNT wall. Table 3 lists peak heights (h_{CH_3} and h_{OH}), and peak positions (d_{CH_3} and d_{OH}) for the RDP-CH_3 and RDP-OH. For ethanol molecules within the (7, 7), (8, 8), (9, 9), and (10, 10) CNTs, all h_{CH_3} are found to be around 6.5. Furthermore, the d_{CH_3} values of these four CNTs are also found to be quite similar. Previous MD simulations have found that the distance between the wall and the peak of RDPs of oxygen molecules[57] and water molecules[56] inside CNTs is similar in different CNTs, which suggests that the distance between the wall and the peak has a close relationship with the force field parameter $\sigma_{site-wall}$. This relationship agrees well with results of methyl groups obtained here. The value of d_{CH_3} (∼0.36 nm) closely matches that of σ_{CH_3-wall} (united-atom model: 0.366 nm; all-atom model: 0.352 nm), implying that the behavior of methyl groups within the nanotube may be determined by wall−fluid interactions.

However, when it comes to hydroxyl groups, d_{OH} and h_{OH} are found to vary significantly with the diameter, as listed in Table 3. The value of d_{OH} of (6, 6) CNT is 0.33 nm, which closely matches with $\sigma_{OH-wall}$. However, it is around 0.49 nm in (10, 10) CNT, nearly 40% larger than $\sigma_{OH-wall}$. Shapes of RDP-OH are also observed to be obviously broadened with the increase of diameter, and h_{OH} decreases from around 8.0 to 3.5. The different variations of RDP-CH_3 and RDP-OH indicate that the determinant factor for the behavior of hydroxyl groups should be different from that of methyl groups. Fluid−fluid interactions might dominate here.

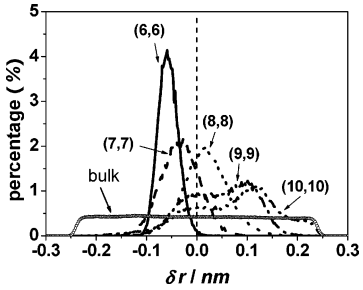

Figure 5. Distributions of the methyl-hydroxyl radial distance within various CNTs. The positive value means methyl groups closer to the wall, whereas the negative value means hydroxyl groups closer to the wall.

Furthermore, we observe that, in the (6, 6) and (7, 7) CNTs, $d_{CH_3} > d_{OH}$, whereas $d_{CH_3} < d_{OH}$ inside the (8, 8), (9, 9), and (10, 10) CNTs. This implies that the methyl and hydroxyl groups have their radial density distributions reorganized as the diameter of nanotube increases.

III.C. Relative Radial Distributions of the Methyl and Hydroxyl Groups of Ethanol Molecules within CNTs. The relative distance of methyl and hydroxyl groups is also found to vary with the diameter of nanotube. We employ the relative radial distance δr, which is calculated by eq 2,

$$\delta r = r_{CH_3} - r_{OH} \tag{2}$$

where r_{CH_3} and r_{OH} are the radial positions of methyl and hydroxyl groups of the same confined ethanol molecule. The positive δr means that the methyl group is closer to the nanotube wall, whereas the negative value means the reverse. Figure 5 shows the distributions of r for ethanol molecules inside CNTs investigated in this study. The distribution of δr for bulk ethanol is also plotted in Figure 5 according to the relative distance of the methyl and hydroxyl groups in the z-direction. Cross-section graphs of ethanol molecules inside CNTs are shown in Figure 6.

From Figure 5, it is observed that δr of the (6, 6) and (7, 7) CNTs is generally negative, implying that polar hydroxyl groups of confined ethanol molecules are generally closer to the nonpolar nanotube wall than the nonpolar methyl groups. This agrees well with the observation that d_{OH} is smaller than d_{CH_3} for these two CNTs, as listed in Table 3. As shown in Figure 6, panels a and b, in the (6, 6) and (7, 7) CNTs, ethanol molecules concentrate in the tube center and form a single file along the axial direction of tube.

However, as shown in Figure 5, majority of δr is positive in CNTs with diameters larger than 1.0 nm, indicating that majority hydroxyl groups of confined ethanol molecules in these tubes locate around the central axis of tube. This is further confirmed by the cross-section graphs shown in Figure 6. Within the (8, 8), (9, 9) and (10, 10) CNTs, methyl groups form a ring-like structure around the nanotube, and hydroxyl groups mainly aggregate within the interior formed by the "methyl ring". Such aggregation could be the consequence of formation of hydrogen bonds. In turn, it implies that fluid−fluid interactions, mainly in the form of hydrogen-bonding interaction, have significant influence on the behavior of hydroxyl groups within the CNTs.

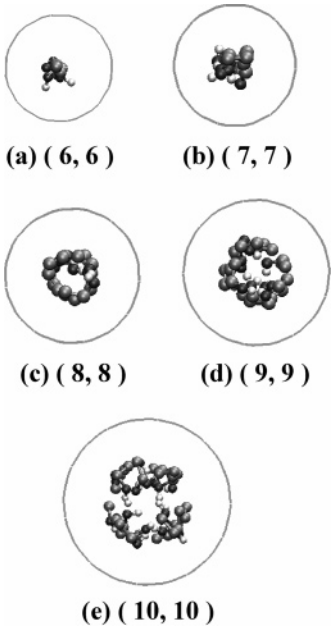

Figure 6. Snapshots of ethanol molecules in various CNTs. Grey ones are carbon atoms of methylene or methyl groups, dark ones are oxygen atoms of hydroxyl groups, and white ones are hydrogen atoms of hydroxyl groups. Hydrogen atoms of the methyl and methylene groups are not shown for clarity.

Furthermore, comparing images shown in Figure 6, it is observed that the structure of ethanol molecules confined in (8, 8) CNT seems to have a certain ordered structure. It is noted that the effective internal diameter of the (8, 8) CNT is 0.731 nm, using 0.35 nm as the diameter of the carbon atoms. It is similar to the size (0.70 nm) of carbon nanopores in which Kaneko et al.[34] found that ethanol molecules have a highly preferred orientation with in situ X-ray diffraction, although the pore shape is a slit in that study and is cylindrical in this work. This implies that orientation of ethanol molecules confined within CNTs may have some special characteristics, which are discussed in detail in the next section.

III.D. Orientation Distributions of Ethanol Molecules in CNTs. The preferred orientation of certain bonds and molecular dipole moments is another characteristic of confined molecules. The preferred dipole orientation of molecules could have fundamental influence on the function of the pore.[58] As addressed, ethanol is an intermediate polar molecule with both nonpolar and polar groups. To better understand the orientation of ethanol molecules within CNTs, we define three angles against the positive direction of the z-axis (tube axial direction): α, β, and θ, between the nonpolar part (CH_3-CH_2), polar part (O−H), and the dipole moment of the ethanol molecule, respectively. Figure 7 illustrates definitions of these three angles.

Figure 8, panels a and b, shows the distributions of cos α within various CNTs gained with the all-atom and united-atom

TABLE 3: Peak Heights (h) and Distances (d) from the CNT Wall of RDP-CH_3 and RDP-OH of Ethanol Molecules within CNTs[a]

	(6, 6)	(7, 7)	(8, 8)	(9, 9)	(10, 10)
d_{CH_3}	0.40 (0.40)	0.37 (0.37)	0.36 (0.36)	0.36 (0.36)	0.36 (0.36)
h_{CH_3}	51.50 (28.71)	6.60 (6.12)	7.17 (6.60)	6.40 (5.70)	6.0 (5.60)
d_{OH}	0.33 (0.34)	0.34 (0.34)	0.39 (0.40)	0.47 (0.46)	0.49 (0.50)
h_{OH}	8.85 (7.33)	5.00(4.71)	4.91 (5.20)	4.16 (3.43)	3.64 (3.22)

[a]The values in the brackets are the results from the united-atom model.

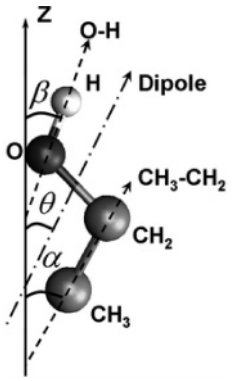

Figure 7. Schematic illustration for definitions of α, β, and θ. Hydrogen atoms of the methyl and methylene groups are not shown for clarity.

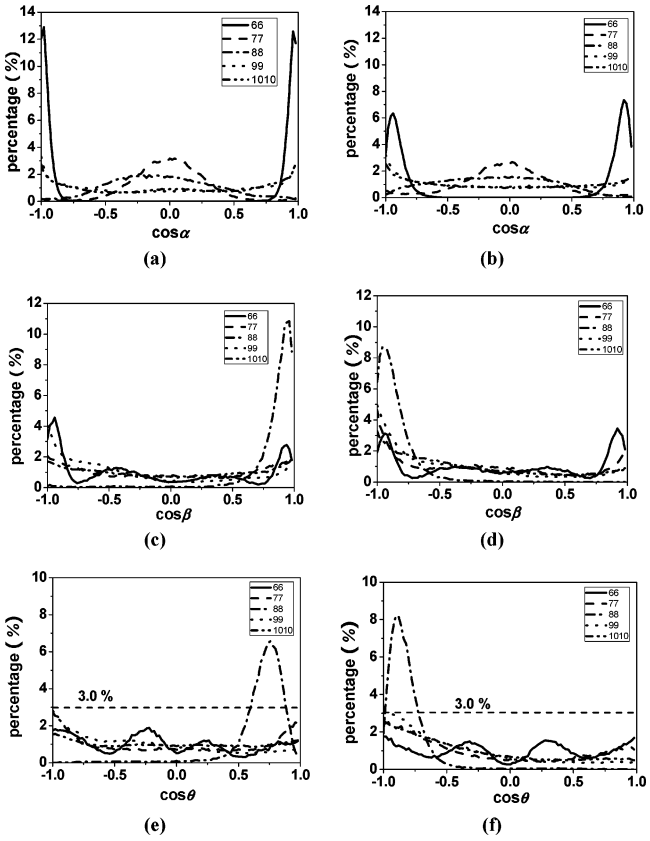

Figure 8. Distributions of cos α, cos β, and cos θ within various CNTs. (a) cos α (all-atom model); (b) cos α (united-atom model); (c) cos β (all-atom model); (d) cos β (united-atom model); (e) cos θ (all-atom model) and (f) cosθ (united-atom model). The peak around −1 or 1 indicates that bonds prefer to align along the axial direction of the tube, whereas the peak around zero means that bonds prefer to align along the radial direction of the tube.

models, respectively, whereas those of cos β are shown in Figure 8, panels c and d, respectively. Values of 1 and −1 mean that the bond aligns along the axial direction, whereas zero indicates that the bond would align along the radial direction of the nanotube. In general, results of united-atom and all-atom models quantitatively agree with each other.

Similar to RDPs, orientation distributions of nonpolar and polar parts also behave differently with the varying diameter of CNTs. As for nonpolar parts, the most concentrated distribution of cos α is found within the narrowest (6, 6) CNT, with two peaks around −1 and 1, indicating that the CH_3-CH_2 bond prefers to align along the axial direction, as shown in Figure 8, panels a and b. With the increase of diameter, the orientation of the CH_3-CH_2 bond in any direction becomes possible, and the distribution becomes even. This monotonic tendency with diameter implies that the orientation of nonpolar parts of ethanol may be determined by the effect of the nanotube wall, consistent with the finding that wall effects determine the behavior of methyl groups, as discussed in Section III.B.

As for O−H bonds, interestingly, the distribution of cos β is found to be most concentrated within the (8, 8) CNT instead of the narrowest (6, 6) CNT, in which ethanol molecules could be confined in, as shown in Figure 8, panels c and d. Within the (8, 8) CNT, peaks are found around −1 (united-atom model) or 1 (all-atom model), indicating that O−H bonds prefer to align along the axial direction. The opposite preferred orientation predicted by the united-atom model and all-atom model may be because the CNT is uncapped at both terminals; therefore, the ethanol molecules could evenly enter the pore of CNT from either side. We might expect that with an extremely long MD run, both the peaks at −1 and 1 should appear and be similar for either model. The similar behavior has been reported for dipoles of water inside CNT in literature. The dipole of water molecules inside the (6, 6) CNT has been reported to have two preferred orientations, either pointing "up" or "down" along the tube axial by Vaitheeswaran et al.[59] with Grand Canonical Monte Carlo (GCMC) simulation, whereas Wang et al.[56] and Huang et al.[24] have observed only one preferred orientation for water in the (6, 6) CNT with MD simulations less than 600 ps. In addition, the single peak indicates that the reorientation of O−H bonds may be extremely rare within the (8, 8) CNT. Although peaks around −1 or 1 could be found within other tubes, their peak heights are much lower, meaning the orientation of O−H bonds within other CNTs of this work is much more random as compared to that within the (8, 8) CNT. The wider distribution also implies that the reorientation of O−H bonds within other CNTs is easier than that in the (8, 8) CNT.

Fluid-fluid interactions may play an important role in such non-monotonic behavior. In general, the confinement effect by CNT would decrease with the increase in diameter. However, it is more complicated for the effect of fluid−fluid interactions. As discussed in Section III.A, for ethanol molecules, $<n_{HB}>$ is bulk-like within (8, 8), (9, 9), and (10, 10) CNTs. Then, the constraints on hydroxyl groups from fluid−fluid interactions within these three tubes are stronger than those within (6, 6) and (7, 7) CNTs, where $<n_{HB}>$ is only half of the bulk value. The two major constraint effects on the orientation of O−H bonds might have different or even reverse tendency with the increase of diameter, which causes the synergistic effect to vary non-monotonically. Although the size of (8, 8) CNT is moderate, the synergistic constraint effect within it might be the strongest, causing the most concentrated orientation. Mashl et al.[22] have found the similar phenomena for water molecules inside CNTs. Their MD simulation showed that water molecules inside a (9, 9) CNT have more ordered structure than those inside other tubes. The fluid−fluid interactions are also found to be critical in this characteristic.

Consequently, the dipole orientation of ethanol molecules within CNTs is extremely sensitive to the diameter. Figure 8, panels e and f, shows the distributions of cos θ in various CNTs with simulation results by all-atom and united-atom models, respectively. Similar to the results of individual bonds, orientation distributions of dipole moment gained from different models quantitatively agree with each other. We observed that cos θ has a highly preferred distribution with a peak around −1 or 1

within the (8, 8) CNT, whereas those in other tubes distribute more evenly from −1 to 1. This means that the dipole orientation would have a highly preferred one within the (8, 8) CNT whose effective internal diameter is 0.731 nm. This confirms the conclusion of Kaneko et al.[34], from X-ray measurement, that the ethanol molecules should have a highly preferred orientation within a carbon nanopore with a size around 0.7 nm. Interestingly, quite different from the observation of water from molecular simulations that the highly preferred dipole orientation could be found within any CNT with a diameter less than 0.811 nm,[56] the highly preferred dipole orientation of ethanol is observed only within the (8, 8) CNT, whose diameter is moderate among the tubes in this study. A slight variation of tube diameter, either an increase or a decrease, could result in the dipole orientation of ethanol molecules altering from highly preferred to random. The opposite preferred dipole orientation of the all-atom and united-atom models should be due to the same reason for the O−H bonds, which was discussed earlier in this work.

Another interesting thing is that both orientations of the dipole and O−H bonds of ethanol molecules within the (8, 8) CNT prefer to align along the axial direction, very similar to the typical feature for the hydrogen-bonded single-file chain of water pointed out by Mann and Hall.[60] Moreover, the average number (1.65) of hydrogen bond per ethanol molecules in the (8, 8) CNT is quit similar to that (1.54) of water molecules within the (6, 6) CNT,[56] in which the single-filed water chains have been observed with molecular simulations.[18] On the basis of these features, we may expect that the ethanol molecules could form a hydrogen-bonded single-file chain within the biological channel.

III.E. Molecular Conformations of Ethanol Molecules in CNTs. Different from water molecules, ethanol molecules have different conformations because of its complicated structure. The hydroxyl group of an ethanol molecule can either be aligned along the methyl group or in one of the two equivalent positions gauche to the methyl group, as illustrated by the Newman projections in Figure 9a. These two types of conformations have different dihedral angles (ϕ) of CH_3-CH_2-O-H: gauche (0°∼120°, 240°∼360°) and trans (120°∼240°). The conformation equilibrium of bulk ethanol is nearly inert to temperature, as shown by the MD simulation results of Saiz et al.[46] However, we find that the confinement can induce remarkable variation of the conformational equilibrium.

Figure 9b shows the distributions of ϕ of ethanol molecules inside (6, 6), (8, 8), and (10, 10) CNTs with simulation results gained by the united-atom model. The distribution of the bulk ethanol is also plotted for comparison. As shown in Figure 9b, the central maximum corresponds to the trans conformation, whereas the other two maxima correspond to the gauche conformations. The profile shapes within different CNTs change significantly, implying that the conformational equilibrium of ethanol would change considerably with the diameter of nanotube. Gulmen et al.[61] also found that the conformational equilibrium of ethylene alcohol in an amorphous nanopore would change considerably because of the confinement. It is surprising to find that the central maximum disappears for ethanol molecules confined in the (8, 8) CNT, which means that the gauche conformations may be the only stable type within this nanotube. The rest trans conformation found may be just the transition state as it changes from one gauche conformation to another.

We integrate the profiles of ϕ within various nanotubes and plotted the proportions of the gauche conformations as a function

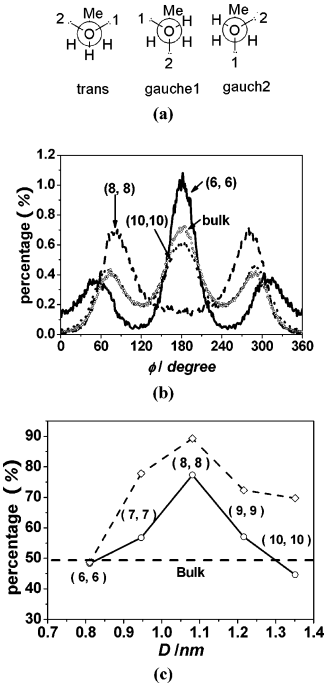

Figure 9. (a) Newman projections of conformations of ethanol molecules. (b) Distributions of CH_2-OH dihedrals of confined ethanol molecules inside (6, 6), (8, 8), and (10, 10) CNTs and bulk ethanol molecules by the united-atom model. (c) The percentage of gauche ethanol inside CNT as a function of tube diameter (D) (○: united-atom model; ◇: all-atom model).

of diameter (D) in Figure 9c. The result of the bulk phase is also shown in Figure 9c for comparison and is found to agree well with the previous simulation results of Jorgensen[43] and Saiz et al.[46] It is found that the results gained from the all-atom model are always larger than those from the united-atom model. Jorgensen[43] suggested that there is probably a small steric preference for hydrogen bonding with a gauche molecule. The "lone-pair" region on oxygen is less encumbered by the nonpolar groups, and the hydroxyl hydrogen is more encumbered for the gauche, rather than the trans, conformation. It is noted that the all-atom model takes more size and energy effects of nonpolar groups into account than the united-atom model does, which may cause more gauche ethanol molecules within the nanotube. Nevertheless, we could find two features for the variation of molecular conformation proportion with diameter in Figure 9c. First, the variation of diameter can induce considerable change of the conformation equilibrium. For instance, the change from (6, 6) to (8, 8) CNTs would result in the proportion of gauche conformations changing from around 50% to more than 75%. Second, as shown in Figure 9c, among the CNTs investigated, the proportion of gauche conformations for confined ethanol molecules is the largest in the (8, 8) CNT, where ethanol molecules are found to have highly preferred dipole orientation.

Recently, several experimental technologies have been developed to distinguish the trans and gauche ethanol. Weibel et al.[62] reported the distinct branch structure on the OH vibrational spectrum of the trans and gauche conformation recorded with photoacoustic absorption spectroscopy. Abu-samha et al.[63] found conformational effects in carbon 1s photoelectron spectra of ethanol. They also gained the theoretical spectrum for the gauche and trans conformations. The observation here implies that, using carbon nanotubes, we may be able to enrich certain conformation for ethanol and better clarify signals for different conformations. Furthermore, the conformation measurement of

confined ethanol molecules might be helpful to further identify the role of ethanol in the biological channel.

IV. Conclusions

Using single-walled armchair carbon nanotubes with diameters ranging from 0.68 to 1.35 nm, we have performed a series of equilibrium MD simulations to investigate the size dependence of the structural characteristics of confined ethanol molecules under ambient conditions. The structural properties investigated include the average number of hydrogen bonds, radial density distributions of methyl and hydroxyl groups, orientation distributions of the methyl-methylene, oxygen−hydrogen bonds and the dipole moment, and molecular conformations by both united-atom and all-atom models. The overall good agreement of the corresponding results indicates that the structural characteristics of the multiatom molecules within the nanometer scale confinement may be well investigated with a united-atom model only if it has been properly parametrized.

It appears that the dipole orientation of confined ethanol molecules depends strongly on diameter. Only inside a (8, 8) CNT, whose diameter is 1.081 nm, did the dipole orientation of confined ethanol molecules preferentially align along the axial direction. A slight variation of the diameter, either a decrease or an increase, would result in the disappearance of this high preference of dipole orientation. Such novel diameter-sensitive dipole orientation is related to the synergistic effect of wall−fluid and fluid−fluid interactions. The different variations of the nonpolar and polar groups with the diameter of nanotube reveal that the wall−fluid interactions determine the behavior of nonpolar groups, whereas the fluid−fluid interactions determine the behavior of polar groups, mainly through the association of hydrogen bonds. Similar to that of water molecules, an obvious decrease of the average number of hydrogen bond only occurs within tubes narrower than 1.0 nm. The increase in diameter may result in the decrease of the wall effect and the enhancement of fluid−fluid interactions, which would bring forth the non-monotonic variation of confinement effect on ethanol molecules with diameter. A (8, 8) CNT might just be the one where the synergistic confinement effect is the strongest. The proportion of molecular conformations also varies considerably with diameter; the highest proportion of gauche conformation corresponds to the high preferred dipole orientation. The findings in this work would shed light on the understanding of molecular behavior of ethanol molecules in nanoporous materials and biological channels.

Acknowledgment. This work was supported by the Joint Research Fund for Young Scholars in Hong Kong and Abroad (No. 20428606), the National Natural Science Foundation of China (Grant Nos. 20246002, 20236010, 20376032, and 20676062), National Basic Research Program of China (No. 2003CB615700), National High Technology Research and Development Program of China (Nos. 2003AA333010 and 2006AA03Z455), and the Key Science Foundation of Jiangsu Province, China (BK 2004215). K. E. G. thanks the fund of the National Science Foundation, through the award CTS-0211792. The authors also acknowledge computer time provided by the College of Computer Engineering and Science, Shanghai University.

References and Notes

(1) Zheng, M.; Jagota, A.; Strano, M. S.; Santos, A. P.; Barone, P.; Chou, S. G.; Diner, B. A.; Dresselhaus, M. S.; McLean, R. S.; Onoa, G. B.; Samsonidze, G. G.; Semke, E. D.; Usrey, M.; Walls, D. J. *Science* **2003**, *302*, 1545.

(2) Liu, C.; Fan, Y. Y.; Liu, M.; Cong, H. T.; Cheng, H. M.; Dresselhaus, M. S. *Science* **1999**, *286*, 1127.

(3) Holt, J. K.; Park, H. G.; Wang, Y.; Stadermann, M.; Artyukhin, A. B.; Grigoropoulos, C. P.; Noy, A.; Bakajin, O. *Science* **2006**, *312*, 1034.

(4) Newsome, D. A.; Sholl, D. S. *Nano Lett.* **2006**, *6*, 2150.

(5) Zhou, Q. L.; Zhou, Q.; Forman, S. A. *Biochemistry* **2000**, *39*, 14920.

(6) Forman, S. A.; Miller, K. W.; Yellen, G. *Mol. Pharmacol.* **1995**, *48*, 574.

(7) Mihic, S. J.; Ye, Q.; Wick, M. J.; Koltchine, V. V.; Krasowski, M. D.; Finn, S. E.; Mascia, M. P.; Valenzuela, C. F.; Hanson, K. K.; Greenblatt, E. P.; Harris, R. A.; Harrison, N. L. *Nature* **1997**, *389*, 385.

(8) Ren, H.; Honse, Y.; Peoples, R. W. *J. Biol. Chem.* **2003**, *278*, 48815.

(9) Vane, L. M. *J. Chem. Technol. Biotechnol.* **2005**, *80*, 603.

(10) Jiang, S. Y.; Rhykerd, C. L.; Gubbins, K. E. *Mol. Phys.* **1993**, *79*, 373.

(11) Maddox, M. W.; Gubbins, K. E. *Langmuir* **1995**, *11*, 3988.

(12) Muller, E. A.; Rull, L. F.; Vega, L. F.; Gubbins, K. E. *J. Phys. Chem.* **1996**, *100*, 1189.

(13) Striolo, A.; Chialvo, A. A.; Cummings, P. T.; Gubbins, K. E. *Langmuir* **2003**, *19*, 8583.

(14) Striolo, A.; Chialvo, A. A.; Gubbins, K. E.; Cummings, P. T. *J. Chem. Phys.* **2005**, *122*, 234712.

(15) Shevade, A. V.; Jiang, S. Y.; Gubbins, K. E. *Mol. Phys.* **1999**, *97*, 1139.

(16) Shevade, A. V.; Jiang, S. Y.; Gubbins, K. E. *J. Chem. Phys.* **2000**, *113*, 6933.

(17) Gelb, L. D.; Gubbins, K. E.; Radhakrishnan, R.; Sliwinska-Bartkowiak, M. *Rep. Prog. Phys.* **1999**, *62*, 1573.

(18) Hummer, G.; Rasaiah, J. C.; Noworyta, J. P. *Nature* **2001**, *414*, 188.

(19) Koga, K.; Gao, G. T.; Tanaka, H.; Zeng, X. C. *Nature* **2001**, *412*, 802.

(20) Bai, J.; Wang, J.; Zeng, X. C. *Proc. Natl. Acad. Sci.* **2006**, *103*, 19664.

(21) Noon, W. H.; Ausman, K. D.; Smalley, R. E.; Ma, J. P. *Chem. Phys. Lett.* **2002**, *355*, 445.

(22) Mashl, R. J.; Joseph, S.; Aluru, N. R.; Jakobsson, E. *Nano Lett.* **2003**, *3*, 589.

(23) de Souza, N. R.; Kolesnikov, A. I.; Burnham, C. J.; Loong, C. K. *J. Condes. Matter Phys.* **2006**, *18*, S2321.

(24) Huang, L. L.; Shao, Q.; Lu, L. H.; Lu, X. H.; Zhang, L. Z.; Wang, J.; Jiang, S. Y. *Phys. Chem. Chem. Phys.* **2006**, *8*, 3836.

(25) Huang, L. L.; Zhang, L. Z.; Shao, Q.; Wang, J.; Lu, L. H.; Lu, X. H.; Jiang, S. Y.; Shen, W. F. *J. Phys. Chem. B* **2006**, *110*, 25761.

(26) Li, J.; Gong, X.; Lu, H.; Li, D.; Fang, H.; Zhou, R. *Proc. Natl. Acad. Sci.* **2007**, *104*, 3687.

(27) Zhang, Q. X.; Zheng, J.; Shevade, A.; Zhang, L. Z.; Gehrke, S. H.; Heffelfinger, G. S.; Jiang, S. Y. *J. Chem. Phys.* **2002**, *117*, 808.

(28) Denis, M.; Regis, G.; Yongde, X.; Christiane, A.-S. *J. Chem. Phys.* **2004**, *121*, 1466.

(29) Guegan, R.; Morineau, D.; Alba-Simionesco, C. *Chem. Phys.* **2005**, *317*, 236.

(30) Sliwinska-Bartkowiak, M.; Dudziak, G.; Sikorski, R.; Gras, R.; Gubbins, K. E.; Radhakrishnan, R. *Phys. Chem. Chem. Phys.* **2001**, *3*, 1179.

(31) Ohkubo, T.; Iiyama, T.; Kaneko, K. *Chem. Phys. Lett.* **1999**, *312*, 191.

(32) Ohkubo, T.; Iiyama, T.; Nishikawa, K.; Suzuki, T.; Kaneko, K. *J. Phys. Chem. B* **1999**, *103*, 1859.

(33) Kaneko, K. *Carbon* **2000**, *38*, 287.

(34) Ohkubo, T.; Kaneko, K. *Colloid Surf. A-Physicochem. Eng. Asp.* **2001**, *187*, 177.

(35) Feller, S. E.; Brown, C. A.; Nizza, D. T.; Gawrisch, K. *Biophys. J.* **2002**, *82*, 1396.

(36) Patra, M.; Salonen, E.; Terama, E.; Vattulainen, I.; Faller, R.; Lee, B. W.; Holopainen, J.; Karttunen, M. *Biophys. J.* **2006**, *90*, 1121.

(37) Hofmann, D.; Fritz, L.; Paul, D. *J. Membr. Sci.* **1998**, *144*, 145.

(38) Takaba, H.; Koyama, A.; Nakao, S. *J. Phys. Chem. B* **2000**, *104*, 6353.

(39) Jia, W.; Murad, S. *Mol. Phys.* **2006**, *104*, 3033.

(40) Striolo, A. *Nano Lett.* **2006**, *6*, 633.

(41) Zhu, F. Q.; Schulten, K. *Biophys. J.* **2003**, *85*, 236.

(42) Jorgensen, W. L. *J. Am. Chem. Soc.* **1981**, *103*, 335.

(43) Jorgensen, W. L. *J. Phys. Chem.* **1986**, *90*, 1276.

(44) Jorgensen, W. L.; Maxwell, D. S.; Tirado-Rives, J. *J. Am. Chem. Soc.* **1996**, *118*, 11225.

(45) Chen, B.; Potoff, J. J.; Siepmann, J. I. *J. Phys. Chem. B* **2001**, *105*, 3093.

(46) Saiz, L.; Padro, J. A.; Guardia, E. *J. Phys. Chem. B* **1997**, *101*, 78.

(47) Erik, J. W. W.; Alex, C. H.; Paul, J. v. M.; David van der, S. *J. Chem. Phys.* **2003**, *119*, 7308.

(48) Stewart, E.; Shields, R. L.; Taylor, R. S. *J. Phys. Chem. B* **2003**, *107*, 2333.

(49) Humphrey, W.; Dalke, A.; Schulten, K. *J. Mol. Graph.* **1996**, *14*, 33.
(50) Lindahl, E.; Hess, B.; van der Spoel, D. *J. Mol. Model.* **2001**, *7*, 306.
(51) Tom, D.; Darrin, Y.; Lee, P. *J. Chem. Phys.* **1993**, *98*, 10089.
(52) Berendsen, H. J. C.; Postma, J. P. M.; Gunsteren, W. F. v.; DiNola, A.; Haak, J. R. *J. Chem. Phys.* **1984**, *81*, 3684.
(53) Ryckaert, J.-P.; Ciccotti, G.; Berendsen, H. J. C. *J. Comp. Phys.* **1977**, *23*, 327.
(54) Luzar, A.; Chandler, D. *Nature* **1996**, *379*, 55.
(55) Gordillo, M. C.; Marti, J. *Chem. Phys. Lett.* **2000**, *329*, 341.
(56) Wang, J.; Zhu, Y.; Zhou, J.; Lu, X. H. *Phys. Chem. Chem. Phys.* **2004**, *6*, 829.
(57) Lee, K. H.; Sinnott, S. B. *Nano Lett.* **2005**, *5*, 793.
(58) Compoint, M.; Boiteux, C.; Huetz, P.; Ramseyer, C.; Girardet, C. *Phys. Chem. Chem. Phys.* **2005**, *7*, 4138.
(59) Vaitheeswaran, S.; Rasaiah, J. C.; Hummer, G. *J. Chem. Phys.* **2004**, *121*, 7955.
(60) Mann, D. J.; Halls, M. D. *Phys. Rev. Lett.* **2003**, *90*, 195503.
(61) Gulmen, T. S.; Thompson, W. H. *Langmuir* **2006**, *22*, 10919.
(62) Weibel, J. D.; Jackels, C. F.; Swofford, R. L. *J. Chem. Phys.* **2002**, *117*, 4245.
(63) Abu-samha, M.; Borve, K. J.; Saethre, L. J.; Thomas, T. D. *Phys. Rev. Lett.* **2005**, *95*, 103002.